

Intranuclear Aggregation of Mutant FUS/TLS as a Molecular Pathomechanism of Amyotrophic Lateral Sclerosis*

Received for publication, September 8, 2013, and in revised form, November 18, 2013 Published, JBC Papers in Press, November 26, 2013, DOI 10.1074/jbc.M113.516492

Takao Nomura^{‡1}, Shoji Watanabe^{§1}, Kumi Kaneko[¶], Koji Yamanaka^{||}, Nobuyuki Nukina^{**}, and Yoshiaki Furukawa^{‡2}

From the [‡]Department of Chemistry, Laboratory for Mechanistic Chemistry of Biomolecules, Keio University, Yokohama, Kanagawa 223-8522, the [§]Graduate School of Brain Science, Doshisha University, Kyoto 619-0225, the [¶]Laboratory for Motor Neuron Disease, RIKEN Brain Science Institute, Wako, Saitama 351-0198, the ^{||}Department of Neuroscience and Pathobiology, Research Institute of Environmental Medicine, Nagoya University, Nagoya, Aichi 464-8601, and the ^{**}Department of Neuroscience for Neurodegenerative Disorders, Juntendo University Graduate School of Medicine, Tokyo 113-8421, Japan

Background: Abnormal accumulation of mutant FUS/TLS is a pathological change in patients with amyotrophic lateral sclerosis (ALS).

Results: A pathogenic mutation, G156E, increases propensities of FUS/TLS for aggregation *in vitro* and *in vivo*.

Conclusion: Intranuclear aggregation of mutant FUS/TLS is a molecular pathomechanism of ALS.

Significance: A loss of functional TLS/FUS in the nucleus will lead to neurodegeneration.

Dominant mutations in *FUS/TLS* cause a familial form of amyotrophic lateral sclerosis (fALS), where abnormal accumulation of mutant FUS proteins in cytoplasm has been observed as a major pathological change. Many of pathogenic mutations have been shown to deteriorate the nuclear localization signal in FUS and thereby facilitate cytoplasmic mislocalization of mutant proteins. Several other mutations, however, exhibit no effects on the nuclear localization of FUS in cultured cells, and their roles in the pathomechanism of fALS remain obscure. Here, we show that a pathogenic mutation, G156E, significantly increases the propensities for aggregation of FUS *in vitro* and *in vivo*. Spontaneous *in vitro* formation of amyloid-like fibrillar aggregates was observed in mutant but not wild-type FUS, and notably, those fibrils functioned as efficient seeds to trigger the aggregation of wild-type protein. In addition, the G156E mutation did not disturb the nuclear localization of FUS but facilitated the formation of intranuclear inclusions in rat hippocampal neurons with significant cytotoxicity. We thus propose that intranuclear aggregation of FUS triggered by a subset of pathogenic mutations is an alternative pathomechanism of FUS-related fALS diseases.

Fused in sarcoma (FUS),³ also called as TLS (1), is a DNA/RNA-binding protein involved in physiological processes

related to RNA metabolism in particular (2–4). Recently, dominant mutations have been identified in the *FUS* gene to cause a familial form of amyotrophic lateral sclerosis (fALS) (5, 6). Wild-type FUS protein is localized mostly in the nucleus of a motor neuron, but a subset of pathogenic mutations in FUS was found to facilitate its cytoplasmic mislocalization (5, 6). Upon mutations, FUS would hence lose its physiological functions performed in the nucleus, possibly contributing to the reduced viability of cells.

As represented in Fig. 1, FUS is composed of several distinct domains: a SYGQ-rich region (SYGQ), RNA recognition motif (RRM), three RGG-rich regions (RGG1, RGG2, and RGG3), and a zinc finger motif (ZnF) (7). FUS is also characterized by its extreme C-terminal sequence motif, R/H/KX_{2–5}PY, which functions as a nuclear localization signal called PY-NLS (8). PY-NLS binds to nuclear import receptor, karyopherin β 2 (Kap β 2), by which FUS usually localizes at the nucleus (8). Notably, the C-terminal region of FUS is a hot spot for pathogenic mutations (Fig. 1), and those C-terminal mutations have been shown to weaken the affinity of FUS with Kap β 2, thereby resulting in the cytoplasmic mislocalization of mutant FUS (9). Despite this, many fALS-causing mutations have been reported also in the N-terminal SYGQ region as well as RGG1 region of FUS (Fig. 1) and did not affect the nuclear localization of FUS at least in cultured cells (10). In addition, to our knowledge, neuropathological and biochemical analysis of spinal cords of fALS patients with those mutations have not been available so far; therefore, it remains unknown if FUS with a mutation in its SYGQ and RGG1 regions undergoes cytoplasmic mislocalization under pathological conditions.

FUS is an intrinsically aggregation-prone protein even without any mutations (11). Given the sequence analysis predicting the high aggregation propensities at the N-terminal SYGQ region of FUS (12), we suspect that pathogenic mutations at the SYGQ region modulate the aggregation kinetics of FUS. In this study, therefore, we have examined the effects of pathogenic mutations at SYGQ and RGG1 regions on the aggregation propensities of FUS proteins. Among the mutations tested (G156E,

* This work was supported by Grants-in-Aid 24111542 (to Y. F.), 23111006 (to K. Y.), 22110004 (to N. N.) for Scientific Research on Innovative Areas, 22240037 for Scientific Research (A) (to N. N.), 25291028 for Scientific Research (B) (to Y. F.), 24657093 for Challenging Exploratory Research (to Y. F.), and 24700391 for Young Scientists (B) (to S. W.) from the Ministry of Education, Culture, Sports, Science and Technology of Japan, grants-in-aid from the Research Committee of CNS Degenerative Diseases, the Ministry of Health, Labour, and Welfare of Japan (to K. Y.), and CREST from Japan Science and Technology Agency (to N. N.).

¹ Both authors equally contributed to this study.

² To whom correspondence should be addressed. Tel.: 81-45-566-1807; Fax: 81-45-566-1697; E-mail: furukawa@chem.keio.ac.jp.

³ The abbreviations used are: FUS, fused in sarcoma; fALS, a familial form of amyotrophic lateral sclerosis; Kap β 2, Karyopherin β 2; DIV, days *in vitro*; MAP2, microtubule-associated protein 2.

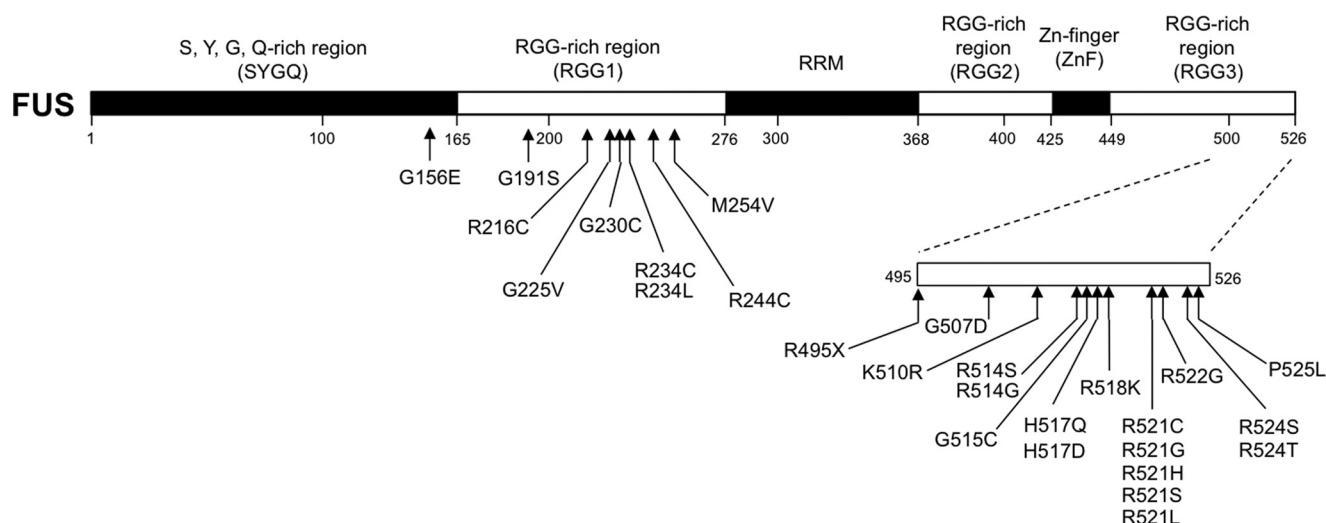


FIGURE 1. **Domain organization of FUS.** FUS is composed of an N-terminal region rich in Ser, Tyr, Gly, and Gln (SYGQ), three regions rich in the RGG sequence (RGG1, RGG2, and RGG3), an RNA recognition motif (RRM), and a zinc finger motif (ZnF). Mutations in FUS causing fALS are also indicated; RGG1 and a C-terminal region of RGG3 are hot spots for pathogenic mutations.

G225V, M254V, and P525L), introduction of the G156E mutation at the SYGQ region was found to render FUS highly prone to aggregation *in vivo* as well as *in vitro*. Such insoluble aggregates exhibited fibrillar morphologies and were capable of triggering the aggregation of wild-type FUS through a seeding reaction. Based upon these results, an alternative pathomechanism of FUS-related fALS has been discussed in which mutations increase the aggregation propensities of FUS proteins.

EXPERIMENTAL PROCEDURES

Preparation of Recombinant FUS Proteins—For preparation of GST-FUS proteins, cDNA of human FUS was cloned in a multiple cloning site (BamHI and SalI) of a vector, pGEX6P-2 (GE Healthcare). A plasmid for expression of GST-FUS-His was prepared by seamlessly inserting six consecutive CAT codons at the C-terminal end of the human FUS coding sequence in the above pGEX6P-2 plasmid containing the GST-FUS gene. Mutations were introduced by the In-Fusion PCR method, and all constructs examined in this study were confirmed by DNA sequencing.

After transfection of a plasmid in *Escherichia coli* (RosettaTM (DE3)), expression of GST-FUS and GST-FUS-His proteins was induced by addition of 0.1 mM isopropyl β -D-thiogalactoside, and the cultures were shaken at 20 °C for 46 h. Cells were lysed in PBS containing 5 mM MgCl₂, 2% Triton X-100, 6.7 mg/liter of DNase I, 0.12 g/liter of lysozyme and a protease inhibitor mixture, cOmplete EDTA-free (Roche Applied Science), and centrifuged to collect soluble supernatant, which was mixed with glutathione-Sepharose 4B resins (GE Healthcare). After being washed with a TN-trehalose buffer (50 mM Tris, 100 mM NaCl, and 200 mM trehalose) at pH 8.0, the resins were treated with a TN-trehalose buffer containing 20 mM reduced glutathione to elute the bound GST-FUS/GST-FUS-His proteins. The eluted GST-FUS-His proteins were then loaded to HisTrap HP column (GE Healthcare) fitted to BioLogic LP (Bio-Rad) and washed with a buffer containing 50 mM Tris, 100 mM NaCl, and 10 mM imidazole, pH 8.0. GST-FUS-His proteins were then eluted from the column by a TN-trehalose buffer with 250 mM

imidazole, pH 6.8 (or 8.0, see text), concentrated by using Vivaspins 15 (MWCO: 10 kDa, Sartorius) and checked by SDS-PAGE. The protein concentration was estimated by using Bio-Rad Protein Assay, in which bovine serum albumin was used as the standard.

Electrophoresis—A sample solution containing 10 μ g of total proteins was mixed with SDS-PAGE sample buffer containing β -mercaptoethanol and loaded on a 10% polyacrylamide gel after boiling for 5 min. Insoluble pellets were re-dissolved in buffer containing 2% SDS and then treated with β -mercaptoethanol before loading on a gel. Following electrophoresis, the gel was stained with Coomassie Brilliant Blue, by which the protein bands were visualized. For Western blotting, the gel was further electroblotted on a 0.2- μ m PVDF membrane (Bio-Rad), where the protein was detected using a mouse monoclonal anti-GST antibody (1:2,000 dilution, Wako) as a primary antibody and a stabilized goat anti-mouse IgG(H+L) peroxidase-conjugated antibody (1:5,000 dilution, Thermo) as a secondary antibody. Blots were developed with ImmunoStar LD (Wako), and images were obtained using Limited-STAGE (AMZ System Science).

Aggregation of Recombinant FUS Proteins—To examine aggregation of FUS, 150 μ l of 5 μ M soluble GST-FUS-His proteins in a TN-trehalose buffer with 250 mM imidazole, pH 6.8, was set in a 96-well plate and left at room temperature. Turbidity was monitored at every 5 min in a plate reader (Epoch, BioTek) by measuring absorbance at 350 nm. After the aggregation reaction for 90 min, the sample was ultracentrifuged at 110,000 $\times g$ for 15 min to prepare soluble supernatant (150 μ l) and insoluble pellets. Pellets were then re-dissolved in 150 μ l of an SDS-PAGE sample buffer, which contains 0.1% SDS and β -mercaptoethanol, and soluble supernatant was also mixed with 5 \times SDS-PAGE sample buffer. Both soluble and insoluble fractions were then boiled and loaded on a 10% SDS-PAGE gel.

For diagnosis of amyloid-like FUS aggregates, 250 μ M thioflavin T was added to the reaction mixture, which was prepared by incubating 5 μ M GST-FUS-His in a TN-trehalose buffer with

250 mM imidazole, pH 6.8, for 2 h at room temperature. Fluorescence spectra (460–600 nm) were then recorded by using F-4500 (HITACHI) with excitation at 442 nm.

Electron microscopic examination of *in vitro* FUS aggregates was also performed. GST-FUS-His aggregates collected with ultracentrifugation at $110,000 \times g$ for 15 min were first adsorbed on STEM100Cu grids coated by elastic carbon (Oken-shoji), washed with pure water, and then negatively stained with 2% phosphotungstic acid. Images were obtained using an electron microscope (TecnaTM Spirit, FEI).

For a seeding reaction, 200 μ l of 5 μ M GST-FUS^{G156E}-His in TN-trehalose buffer with 250 mM imidazole, pH 6.8, was incubated at room temperature for 2 h, and the resultant aggregates were collected with ultracentrifugation at $110,000 \times g$ for 15 min and then resuspended in 20 μ l of TN-trehalose buffer, pH 6.8. After being sheared with ultrasonication, 1.5 μ l of the aggregates was added to 150 μ l of 5 μ M GST-FUS-His in TN-trehalose buffer with 250 mM imidazole, pH 6.8, and incubated at room temperature without any agitation. Turbidity of the reaction mixture was monitored at every 5 min in a plate reader (Epoch, BioTek) by measuring absorbance at 350 nm.

DNA Constructs, Cell Culture, and Transfection—A vector, pCMV-HA or pCMV-myc (Clontech), was used for the construction of plasmids expressing HA-tagged or myc-tagged human FUS, respectively, by utilizing its multiple cloning site (SalI/NotI). Mutations were introduced by QuikChange mutagenesis (Stratagene).

Human neuroblastoma SH-SY5Y cells were maintained in DMEM/F-12 (Invitrogen) with 10% fetal bovine serum (FBS) in 5% (v/v) CO₂ at 37 °C. For immunostaining experiments, cells were seeded on a 4-well chamber slide (Lab-Tek II Chamber Slide with a cover CC2 glass slide, Nalge Nunc international). Cells were transfected with plasmids using Lipofectamine 2000 (Invitrogen) according to the manufacturer's instructions. After transfection for 4 h, culture media were replaced with Neurobasal medium (Invitrogen) supplemented with B-27 supplement (Invitrogen), 500 μ M L-glutamine, and 5 mM N⁶,2'-O-dibutyryl cAMP (Nacalai Tesque) for differentiating SH-SY5Y cells. Following further incubation for 15 h, cells were fixed and immunostained as mentioned below.

Pure neuronal cells were prepared from embryonic rat hippocampus (E18) with a previous method (13) using a poly-L-lysine-coated coverslip. Primary cultured neurons were then grown and maintained in serum-free neuronal maintenance medium containing minimal essential medium (Nacalai tesque), 1 mM sodium pyruvate (Invitrogen), 0.6% glucose (Nacalai tesque), N2 supplement, and 1% B27 supplement (Life Technologies) (14). Neurons were transiently transfected with plasmids by using Lipofectamine 2000 (Invitrogen) at 7 DIV. Transfected neurons were further incubated for 2 days at 37 °C with 5% CO₂ in neuronal maintenance medium.

Immunocytochemistry—For immunostaining of HA-FUS proteins, cultured SH-SY5Y cells were fixed with 4% paraformaldehyde containing 0.12 M sucrose in PBS for 10 min, permeabilized with 0.5% Triton X-100 in PBS for 5 min, and blocked with 0.1% BSA in PBS for 30 min. Cells were then incubated with anti-HA-fluorescein, High Affinity (3F10) (1:100 dilution, Roche Applied Science) in PBS containing 0.1% BSA

for 1 h, washed once with 0.1% Triton X-100 in PBS and twice with 0.1% BSA in PBS. Nuclei were counterstained with DAPI (1:3000 dilution, Molecular Probes).

Transfected neurons at 9 DIV were fixed with 4% paraformaldehyde containing 4% sucrose in Mg²⁺ and Ca²⁺-free Dulbecco's phosphate-buffered saline for 15 min at room temperature, and then blocked with 4% skim milk in TBS containing 0.1% Triton X-100 for 1 h. These neurons were probed with rabbit anti-HA tag polyclonal antibody (MBL), mouse anti-Myc tag monoclonal antibody (clone My3, MBL), and mouse anti-MAP2 monoclonal antibody (clone AP-20, Sigma) for 2 h at room temperature and then further incubated with the corresponding secondary antibodies conjugated with Alexa Fluor 594 or Alexa Fluor 488 (Invitrogen) for 1 h at room temperature. Nuclei were counterstained with bisbenzimidazole H33342 fluorochrome trihydrochloride (Hoechst 33342, Nacalai tesque). Confocal images with a slice thickness of $\sim 1 \mu$ m were obtained by a laser-scanning microscope of the LSM5 Exciter system (Carl Zeiss, Germany) using a $\times 40$ objective lens for SH-SY5Y cells and by Axiovert 200M microscope (ZEISS) with a $\times 40$ and $\times 63$ objective lens for primary neurons.

RESULTS

Purification of Recombinant Full-length FUS Proteins in a Dual Tag System—In a previous studies (e.g. Ref. 15), recombinant FUS was overexpressed in *E. coli* as a GST-fused protein, and we thus first attempted to purify GST-fused FUS proteins (GST-FUS) by affinity chromatography using glutathione (GSH)-Sepharose resins. Although most of GST-FUS proteins were detected in insoluble pellets after lysis of *E. coli* cells, a soluble fraction of the lysates was treated with GSH-Sepharose resins, by which a soluble form of GST-FUS was obtained (Fig. 2A). The purified GST-FUS samples, however, exhibited the absorption peak centered at 260 nm (Fig. 2B), suggesting the contamination of nucleic acids. Indeed, washing the resins with a buffer containing 1 M NaCl can remove the species with the absorption at 260 nm (Fig. 2, B and C), which were digested with RNase but not DNase (Fig. 2D). Accordingly, GST-FUS tightly binds endogenous RNAs in *E. coli*, consistent with a physiological role of FUS as an RNA-binding protein.

Even after removal of bound RNAs, it should also be noted that the purified GST-FUS samples are not homogenous but contain impurities with smaller molecular weight (Fig. 2A). Assuming that these smaller proteinaceous species were bound to GSH-Sepharose, the purified GST-FUS samples were considered to contain significant amounts of the proteins truncated in the middle of FUS. To prepare the recombinant protein containing a full-length sequence of FUS, therefore, we have introduced a polyhistidine (His₆) tag at the C terminus of FUS in addition to the N-terminal GST tag (GST-FUS-His). Similar to the case in GST-FUS, GST-FUS-His was mostly detected in insoluble pellets after cell lysis (Fig. 3A), and incubation of soluble supernatant with GSH-Sepharose resins isolated truncated as well as full-length GST-FUS-His proteins (Fig. 3A). By utilizing the C-terminal His₆ tag in GST-FUS-His, we have further performed Ni²⁺-affinity chromatography and removed the truncated proteins that lack a His₆ tag. A single major band corresponding to the molecular mass of full-length GST-FUS-

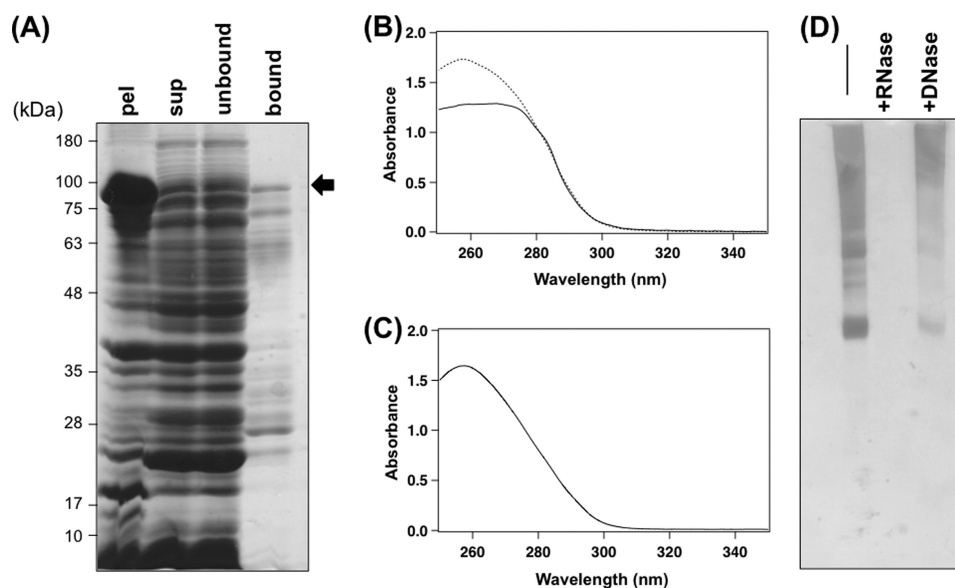


FIGURE 2. Purified GST-FUS proteins associate with *E. coli* endogenous RNAs. A, purification of GST-FUS with GSH-Sepharose resins is examined by SDS-PAGE. *E. coli* cells overexpressing GST-FUS were lysed and then fractionated by centrifugation into soluble supernatant (*sup*) and insoluble pellets (*pel*). The supernatant was treated with GSH-Sepharose resins and separated into the fraction unbound and bound to the resins (*unbound* and *bound*, respectively). A band corresponding to GST-FUS is indicated by an arrow. B and C, examination on the purification of GST-FUS proteins with UV-visible absorption spectroscopy. GSH-Sepharose resins binding GST-FUS proteins were washed with a buffer containing 0.1 M NaCl (*dotted curve*) or 1 M NaCl (*solid curve*), and then the bound GST-FUS proteins were eluted from the resins and examined with UV-visible spectrophotometer (B). The spectrum of the solution washed out with a buffer containing 1 M NaCl was also shown in C. D, *E. coli* endogenous nucleic acids bound to GST-FUS were dissociated by washing GSH-Sepharose resins with a buffer containing 1 M NaCl (see B and C). After treatment with either RNase or DNase, the washes were analyzed with urea-PAGE.

His (about 81 kDa) was confirmed with SDS-PAGE (Fig. 3A) and Western blotting analysis (Fig. 3B). Furthermore, purification of GST-FUS-His using Ni^{2+} -affinity chromatography was found to remove contaminants of nucleic acids (Fig. 3C). These results have, therefore, indicated that a full-length FUS protein without bound nucleic acids was successfully prepared with the two-step purification procedure utilizing N-terminal GST and C-terminal His₆ tags.

A Pathogenic G156E Mutation Increases the Aggregation Propensities of FUS—After being eluted from Ni^{2+} -affinity chromatography resins with an imidazole-containing buffer at pH 8.0, purified GST-FUS-His proteins were concentrated by a centrifugal concentrator to prepare 5 μM solution. The sample solution was, however, found to gradually become turbid when left at 25 °C (Fig. 3D), and almost all GST-FUS-His proteins after incubation for 1 h were detected as insoluble pellets after ultracentrifugation (Fig. 3D, inset). Just after being eluted from the resins, GST-FUS-His proteins started to aggregate, but several procedures including determination of the protein concentration were required for the aggregation assay. It is, therefore, difficult to characterize the aggregation reaction with reproducible kinetic parameters. This is also the case with GST-FUS-His proteins with ALS-causing mutations. In contrast, when the pH of an elution buffer was decreased from 8.0 to 6.8, we serendipitously found no change in the solution turbidity of purified GST-FUS-His even after incubation for 1 h, and GST-FUS-His proteins remained in soluble supernatant after ultracentrifugation (Fig. 3D). Although a detailed mechanism of FUS aggregation still remains obscure, a solution pH appears to be a critical factor affecting the aggregation propensities of our FUS proteins.

We have then tested effects of pathogenic mutations (G156E (16), G225V (17), and M254V (18)) on the aggregation propensity of GST-FUS-His, pH 6.8. As shown in Fig. 4A, no change in the solution turbidity of GST-FUS-His was observed with G225V and M254V mutations (FUS^{G225V}, FUS^{M254V}), but the G156E mutation in GST-FUS-His (FUS^{G156E}) increased solution turbidity, suggesting the formation of aggregates. GST-FUS-His with a pathogenic mutation at the C-terminal region, P525L (5), did not form aggregates and remained soluble at pH 6.8 within the incubation time examined here (Fig. 4, A and B), consistent with limited roles of C-terminal mutations in the aggregation propensities of FUS (15). It is notable that the solution turbidity of FUS^{G156E} increased just after the sample was set in a 96-well plate; therefore, we have speculated that aggregation of FUS^{G156E} already starts when eluted from the resins. In our experimental protocol, it usually required approximately 40 min for starting the turbidity measurement after elution of FUS proteins from the Ni^{2+} -affinity chromatography resins. Indeed, the sample solution of FUS^{G156E} was sometimes already turbid when the sample was set for turbidity measurements; therefore, the initial time point of the FUS^{G156E} aggregation remains obscure. Despite this, FUS^{G156E} was found as insoluble pellets after ultracentrifugation, whereas FUS^{G225V} and FUS^{M254V} remained in soluble supernatant (Fig. 4B). These data have thus clearly shown a distinct role of G156E mutation in increasing the aggregation propensities of a FUS protein at least in the physiological range of solution pH. Notably, furthermore, G144E, G154E, and G156D, which have not been reported as pathogenic mutations, also increased the aggregation propensities of FUS albeit to a lesser extent compared with G156E (Fig. 4B). It is thus likely that the introduction of a neg-

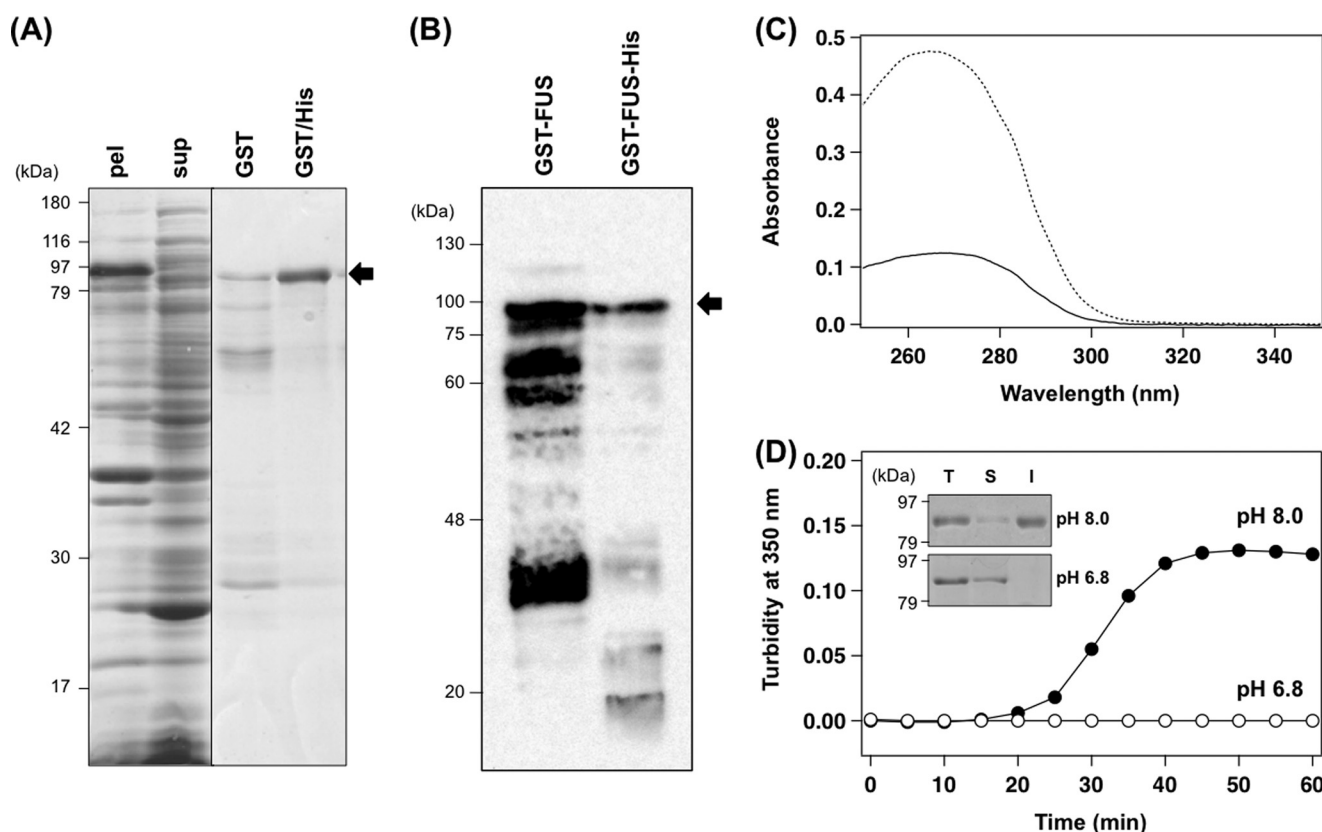


FIGURE 3. Purification and aggregation of GST-FUS-His proteins. A, *E. coli* cells overexpressing GST-FUS-His were lysed and then fractionated by centrifugation into soluble supernatant (*sup*) and insoluble pellets (*pel*). GST-FUS-His in the supernatant fraction was purified with GSH-Sepharose resins (GST) and then with Ni²⁺-affinity chromatography (GST/His). Samples were analyzed by SDS-PAGE using a 10% polyacrylamide gel stained with Coomassie Brilliant Blue. A band corresponding to GST-FUS-His protein was indicated by an arrow. B, Western blotting analysis of purified GST-FUS and GST-FUS-His proteins was performed by using anti-GST antibody. Full-length GST-FUS and GST-FUS-His are indicated by arrows. A GST-FUS sample was found to contain several forms of GST-FUS in which FUS was truncated, whereas most of such truncated proteins were successfully removed in a GST-FUS-His sample. C, UV-visible spectrometric analysis of 10 μ g GST-FUS-His quantified by a Bradford assay was performed after purification with GSH-Sepharose resins (dotted curve) and then further with Ni²⁺-affinity chromatography (solid curve). D, 5 μ M GST-FUS-His in a TN-trehalose buffer with 250 mM imidazole at pH 8.0 (filled circles) or 6.8 (open circles) was incubated at room temperature, and the solution turbidity was monitored by measuring the absorption at 350 nm. Inset, after incubation for 2 h, sample solutions (T) were fractionated into soluble supernatant (S) and insoluble pellets (I) by ultracentrifugation and analyzed by SDS-PAGE using 10% polyacrylamide gel. GST-FUS-His was found to form insoluble aggregates at pH 8.0 but not at pH 6.8.

ative charge to the SYGQ domain contributes to the increase in aggregation propensities of FUS proteins.

FUS Aggregates Exhibit Amyloid-like Properties—Abnormal accumulation of FUS-positive cytoplasmic inclusions have been characterized as a major pathological change in FUS-related fALS cases (5, 6), albeit no report in fALS cases with G156E-mutant FUS. Ultrastructural analysis on those pathological inclusions has further revealed the presence of fibrillar FUS aggregates (19, 20). Consistent with such molecular pathologies, insoluble FUS^{G156E} aggregates in this study (Fig. 4B) were found to possess fibrillar morphologies with approximately 10 nm of the width (Fig. 4C). These structures were not observed in wild-type GST-FUS-His proteins (FUS^{WT}), which remained soluble at pH 6.8 (Fig. 4B). We have also found that the aggregates of FUS^{G156E} increase the fluorescence intensity of thioflavin T, a diagnostic dye of amyloid-like protein aggregates (Fig. 4D). Again, FUS^{WT} did not increase the thioflavin T fluorescence after incubation for 1 h. Pathological inclusions containing FUS in patients with frontotemporal lobar degeneration were not stained with thioflavin dyes (21), but there have been no detailed studies examining reactivity of thioflavin dyes to inclusions in patients with fALS-causing mutations in FUS.

Taken together, the G156E mutation is considered to trigger the formation of fibrillar amyloid-like aggregates of FUS proteins *in vitro*.

G156E Mutation Facilitates Formation of Intracellular FUS-positive Foci in Cells—We next tested if the G156E mutation leads to aggregation of FUS in the intracellular environment. Although FUS appears to shuttle between the nucleus and cytoplasm (4), immunocytochemistry has revealed intracellular localization of wild-type FUS predominantly to the nucleus (10, 22, 23). In differentiated human neuroblastoma SH-SY5Y cells, we have confirmed the nuclear localization of endogenous FUS proteins (data not shown) as well as the transiently transfected human wild-type FUS with an N-terminal HA tag (HA-FUS^{WT}); furthermore, intranuclear inclusions/foci were not observed (Fig. 5A). As reported previously, cytoplasmic staining (including diffuse and foci) of FUS was evident in almost all cells overexpressing HA-FUS with R522G and P525L mutations (Fig. 5, D and E), which is consistent with roles of the C-terminal region as a nuclear localization signal (10, 22, 23). In contrast, HA-FUS with the G156E mutation (HA-FUS^{G156E}) remained nuclear but notably formed intranuclear foci in transfected cells (approximately 40% of

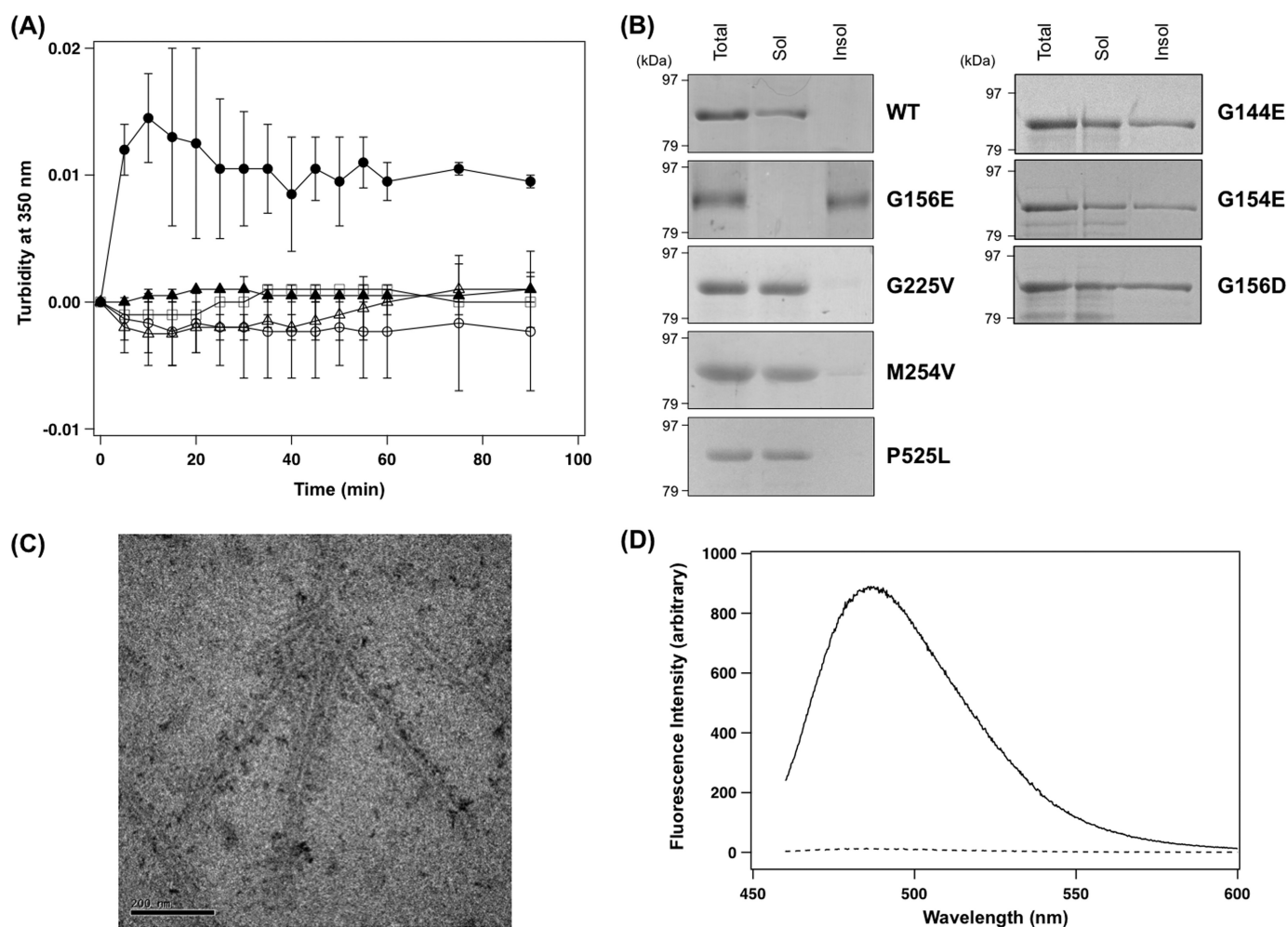


FIGURE 4. G156E mutation facilitates the formation of insoluble aggregates of GST-FUS-His. *A*, 5 μ M GST-FUS-His in a TN-trehalose buffer with 250 mM imidazole, pH 6.8, was incubated at room temperature, and the solution turbidity was monitored by measuring the absorption at 350 nm: wild-type (open circles), G156E (filled circles), G225V (open triangles), M254V (filled triangles), and P525L (open square). *B*, after incubation for 2 h, the samples were collected, fractionated into soluble supernatant (Sol) and insoluble pellets (Insol) by ultracentrifugation and then analyzed by SDS-PAGE using 10% polyacrylamide gel. *C*, insoluble pellets collected from the GST-FUS^{G156E}-His sample incubated for 2 h were examined by an electron microscope after negative staining. A bar at the lower left represents 200 nm. *D*, after incubation for 2 h, 5 μ M GST-FUS-His in TN-trehalose buffer with 250 mM imidazole, pH 6.8, was mixed with 25 μ M thioflavin T and then examined by fluorescence spectrometry: GST-FUS^{WT}-His (broken curve) and GST-FUS^{G156E}-His (solid curve).

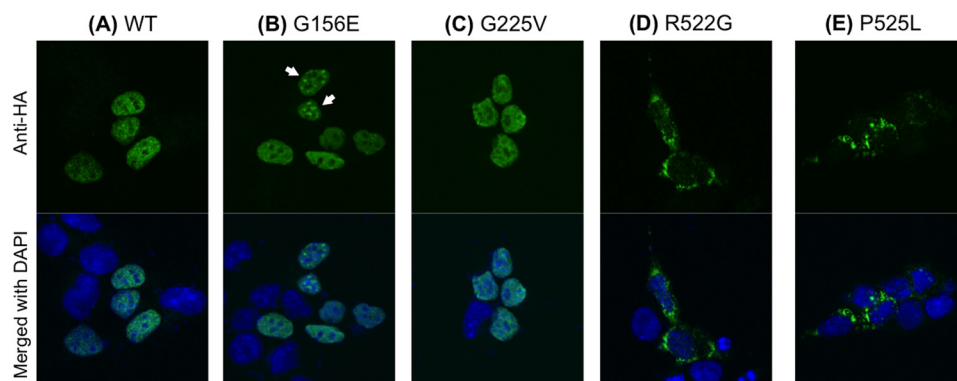


FIGURE 5. Intracellular localization of wild-type and mutant FUS in SH-SY5Y cells. SH-SY5Y cells were first transfected with HA-FUS with the indicated mutations: *A*, WT; *B*, G156E; *C*, G225V; *D*, R522G; *E*, P525L. After differentiation and incubation overnight, the cells were fixed, stained with anti-HA-fluorescein antibody (green), and observed using a confocal microscope. Merged images with nuclei counterstained by DAPI (blue) were also shown in the lower panels. Intranuclear foci observed in cells expressing HA-FUS^{G156E} were indicated with arrows.

total cells expressing HA-FUS^{G156E}, white arrows in Fig. 5*B*). The G225V mutation appears to have minimal effects on both intracellular localization and foci formation of FUS (Fig. 5*C*). Given increased propensities of FUS aggregation *in*

vitro with G156E but not the G225V mutation, these observations using cultured cells support our idea that the G156E mutation facilitates aggregation of FUS even in the intranuclear environment.

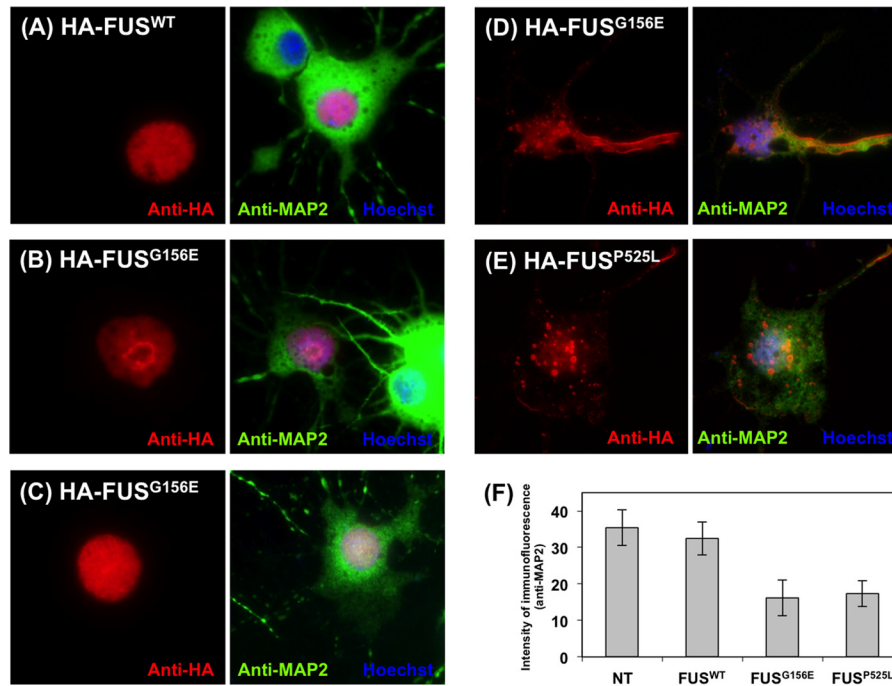


FIGURE 6. FUS^{G156E} forms intranuclear inclusions in rat hippocampal primary neurons. A–E, rat hippocampal primary neurons at DIV 7 were transfected with a plasmid for expression of HA-FUS^{WT} (A), HA-FUS^{G156E} (B–D), or HA-FUS^{P525L} (E) and incubated for 2 days at 37 °C. Cells were fixed, stained with anti-HA (red) and anti-MAP2 (green) antibodies, and observed using a confocal microscope. Nuclei were counterstained with Hoechst 33342. In each panel, the image immunostained with anti-HA antibody (magnification: $\times 63$) and the merged images (magnification: $\times 40$) are shown at the left and right, respectively. F, mean intensity of immunofluorescence observed by staining with anti-MAP2 antibody was measured in a cell body with Image J software and found to significantly decrease when HA-FUS with pathogenic mutations were expressed in cells. Measurements were performed in 15, 12, 18, and 6 cells for NT (non-transfected cells), and cells expressing HA-FUS^{WT}, HA-FUS^{G156E}, and HA-FUS^{P525L}, respectively.

We have also examined effects of pathogenic mutations on FUS proteins in primary neurons. Rat hippocampal primary neurons (DIV 7) were transfected with plasmids for overexpression of HA-FUS proteins and immunostained with anti-HA antibodies after incubation for 2 days (DIV 9). As shown in Fig. 6A, HA-FUS^{WT} was localized in the nucleus with no cytoplasmic staining, whereas HA-FUS^{P525L} formed cytoplasmic foci in primary neurons (Fig. 6E), again confirming critical roles of the C-terminal region as a nuclear localization signal (10, 22, 23). As observed in SH-SY5Y cells, HA-FUS^{G156E} was localized in the nucleus, but notably, abnormal intranuclear structures such as ring-like inclusions (Fig. 6B) and small dot-like foci (Fig. 6C) were evident in primary neurons at DIV 9 expressing HA-FUS^{G156E} but not HA-FUS^{WT} (Fig. 6A). In a subset of transfected neurons, furthermore, HA-FUS^{G156E} was found to form cytoplasmic foci (Fig. 6D), even though Gly¹⁵⁶ appears to play limited roles in the intracellular localization of FUS in SH-SY5Y (Fig. 5) and HeLa cells (10). This could be described by increased aggregation propensities of FUS with the G156E mutation, which result in the formation of foci before being transported into the nucleus.

As shown in Fig. 6, A–E, primary neurons were immunostained with anti-MAP2 (microtubule-associated protein 2) antibodies for visualization, because microtubules help determine the shape and size of neurons (24). Notably, primary neurons expressing HA-FUS^{G156E} and HA-FUS^{P525L} appear to exhibit reduced immunoreactivity toward MAP2 compared with the neurons expressing HA-FUS^{WT} as well as non-transfected neurons (Fig. 6, A–E). Indeed, quantification has revealed a significant decrease in the intensity of immuno-

staining for MAP2 by transfecting cells to overexpress HA-FUS^{G156E} and HA-FUS^{P525L} but not HA-FUS^{WT} (Fig. 6F). Loss of MAP2 has been considered as an early marker for neuronal damage following cerebral ischemia (25), spinal cord injury (26), and traumatic brain injury (27); therefore, potential toxicities of FUS^{G156E} and FUS^{P525L} to neurons would be reflected by reduced intensity of MAP2 immunostaining in primary neurons. In addition, primary neurons expressing HA-FUS^{G156E} and HA-FUS^{P525L} often exhibited abnormal cell shapes (e.g. Fig. 6D) that were characterized by less numbers of dendrites than those of non-transfected cells as well as cells expressing HA-FUS^{WT}, albeit difficult to be quantified. These observations are considered to support toxic roles of FUS^{G156E} and FUS^{P525L} in neurons.

Seeded Aggregation of Wild-type FUS with G156E Mutant FUS in Vitro and in Vivo—It remains obscure how the G156E mutation in FUS exerts toxicity toward neurons, but physiological functions of FUS such as translational and splicing regulations are well expected to be retarded upon formation of aggregates in the nucleus. Notably, neurodegenerative diseases including FUS-related ALS are characterized by their rapid progression after the disease onset, which appears to be regulated by a “seeding reaction” at a molecular level (28). A seeding reaction is an important feature of amyloid-like fibrillar aggregates, in which a piece of protein fibrils can function as a structural template (called as a seed) for facilitating the fibrillation of as-yet-unaggregated protein molecules (29). Once mutant FUS proteins form aggregates in the nucleus, therefore, a seeding reaction could effectively transform the soluble functional FUS into insoluble aggregates, resulting in the progressive dysfunc-

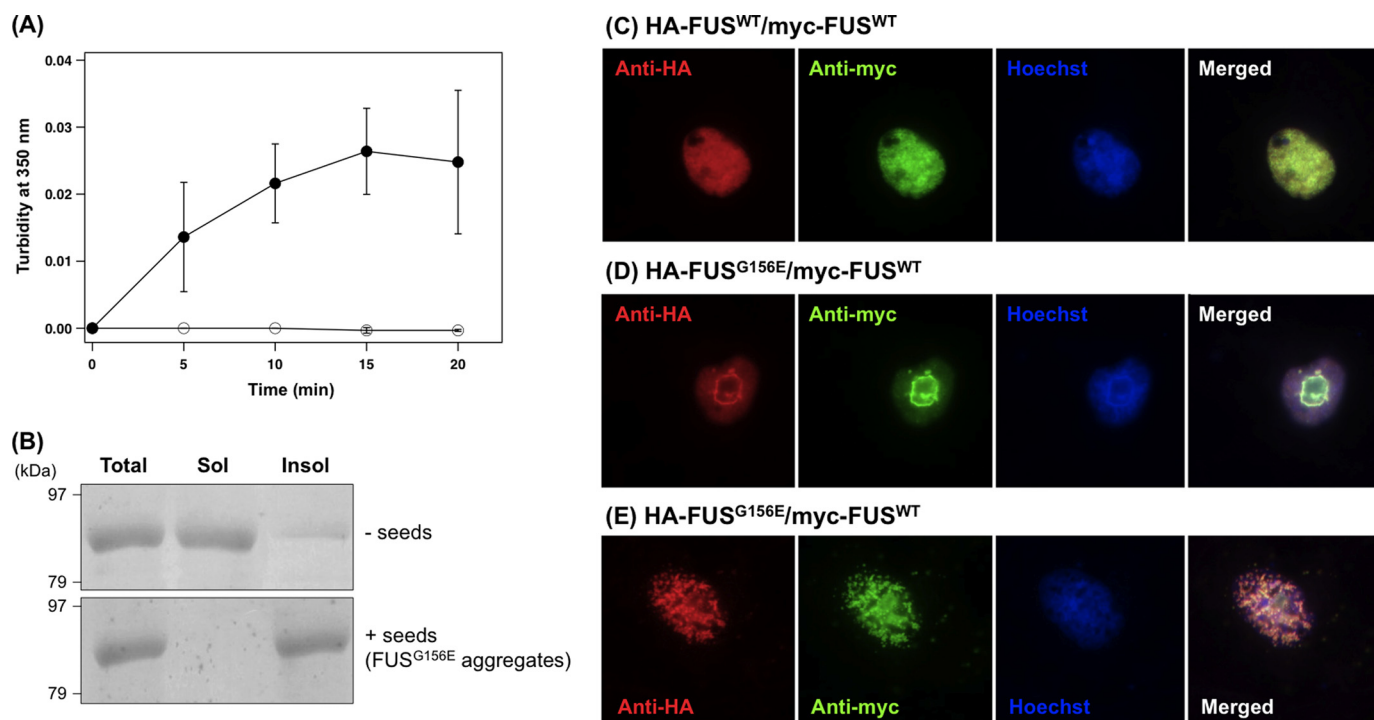


FIGURE 7. A seeded aggregation of wild-type FUS protein with aggregates of FUS^{G156E} *in vitro* and *in vivo*. *A*, 0.5 μ M (monomer-based concentration) GST-FUS^{G156E}-His aggregates were added to 5 μ M GST-FUS^{WT}-His in a TN-trehalose buffer with 250 mM imidazole, pH 6.8 (10% seeding), and then the solution turbidity was monitored by measuring the absorbance at 350 nm (filled circles). Without addition of seeds (GST-FUS^{G156E}-His aggregates), GST-FUS^{WT}-His did not form aggregates (open circles). *B*, after incubation for 20 min in *A*, the GST-FUS^{WT}-His samples with and without GST-FUS^{G156E}-His seeds were fractionated into soluble supernatant (Sol) and insoluble pellets (Insol) by ultracentrifugation and then analyzed by SDS-PAGE using 10% polyacrylamide gel. *C–E*, rat hippocampal primary neurons at DIV 7 were transfected with a plasmid for expression of myc-FUS^{WT} together with a plasmid for expression of HA-FUS^{WT} (*C*) or HA-FUS^{G156E} (*D* and *E*) and incubated for 2 days at 37 °C. Cells were fixed, stained with anti-HA (red) and anti-myc (green) antibodies, and observed using a confocal microscope. Nuclei were counterstained with Hoechst 33342.

tion of FUS with cytotoxicity. Indeed, a seeded fibrillation of proteins has been increasingly noticed as a molecular pathomechanism that describes progression of several neurodegenerative diseases (28).

To test the seeding ability of our FUS^{G156E} aggregates *in vitro*, we have added well sheared FUS^{G156E} aggregates with ultrasonication to the solution containing aggregation-resistant GST-FUS^{WT}-His at pH 6.8. As shown in Fig. 7A, no increase in the turbidity of FUS^{WT}-containing solution was confirmed in the absence of any seeds, but addition of small amounts (10%) of sheared FUS^{G156E} aggregates immediately made the solution turbid, suggesting the seeded aggregation of FUS^{WT} with FUS^{G156E} aggregates. Ultracentrifugal fractionation has further confirmed that almost all FUS^{WT} molecules are detected in insoluble pellets by addition of FUS^{G156E} aggregates (Fig. 7B). Based upon these results, the G156E mutation will increase the propensities of FUS proteins for fibrillar aggregation, which would further facilitate the aggregation of wild-type FUS via a seeding mechanism.

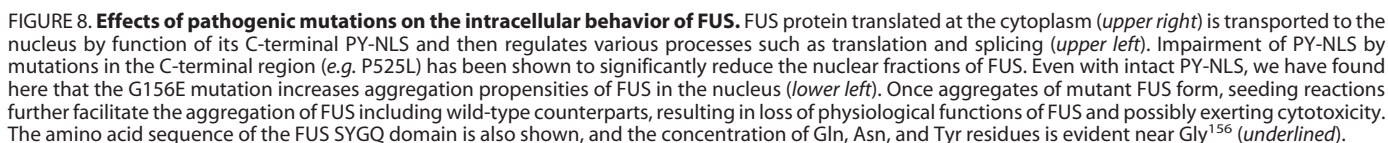
We further examined our seeding mechanism by co-transfection of rat hippocampal primary neurons with plasmids expressing Myc-tagged FUS^{WT} (myc-FUS^{WT}) and HA-FUS. As shown in Fig. 7C, co-expression of myc-FUS^{WT} and HA-FUS^{WT} did not result in the formation of any inclusions, and both wild-type FUS proteins remained diffused in the nucleus. In contrast, when myc-FUS^{WT} was expressed together with HA-FUS^{G156E} in neurons, HA-FUS^{G156E} formed intranuclear structures of ring-like inclusions (Fig.

7D) and dot-like foci (Fig. 7E), and importantly, myc-FUS^{WT} was also detected in those abnormal structures (Fig. 7, D and E). Based upon these results, intranuclear aggregates of FUS^{G156E} can recruit wild-type FUS proteins into their own structures, consistent with a seeding ability of FUS^{G156E} aggregates *in vitro*. A seeded aggregation would, therefore, accelerate the functional impairment of intranuclear FUS proteins.

DISCUSSION

As described in the original paper reporting the G156E mutation in FUS (16), Gly¹⁵⁶ located in the SYGQ domain is evolutionarily conserved among vertebrates, implying an important role in physiological functions of FUS. A low complexity region such as the SYGQ domain of FUS has been proposed as an interaction site with partner proteins (30, 31); therefore, the G156E mutation might perturb protein-protein interactions, eventually exerting cytotoxic effects on motoneurons.

Alternatively, as we have shown here, the G156E mutation, but not the other mutations tested (G225V, M254V, and P525L), increases the aggregation propensity of FUS (Fig. 8). The SYGQ domain of FUS has been predicted to exhibit a prion-forming propensity by using several computer simulations (12). Particularly, Gly¹⁵⁶ locates at the middle of a sequence composed exclusively of Gln, Asn, and Tyr residues (Fig. 8). Several precedents including yeast prion protein, Sup35, have shown high fibrillation propensities of polypeptides rich in Gln, Asn, and Tyr. Although it is still unclear why a



Acknowledgment—We thank Prof. Hiroaki Misonou for helping with experiments on rat primary culture.

REFERENCES

- Crozat, A., Aman, P., Mandahl, N., and Ron, D. (1993) Fusion of CHOP to a novel RNA-binding protein in human myxoid liposarcoma. *Nature* **363**, 640–644
- Uranishi, H., Tetsuka, T., Yamashita, M., Asamitsu, K., Shimizu, M., Itoh, M., and Okamoto, T. (2001) Involvement of the pro-oncoprotein TLS (translocated in liposarcoma) in nuclear factor- κ B p65-mediated transcription as a coactivator. *J. Biol. Chem.* **276**, 13395–13401
- Yang, L., Embree, L. J., Tsai, S., and Hickstein, D. D. (1998) Oncoprotein TLS interacts with serine-arginine proteins involved in RNA splicing. *J. Biol. Chem.* **273**, 27761–27764
- Zinszner, H., Sok, J., Immanuel, D., Yin, Y., and Ron, D. (1997) TLS (FUS) binds RNA *in vivo* and engages in nucleocytoplasmic shuttling. *J. Cell Sci.* **110**, 1741–1750
- Kwiatkowski, T. J., Jr., Bosco, D. A., Leclerc, A. L., Tamrazian, E., Vandenberg, C. R., Russ, C., Davis, A., Gilchrist, J., Kasarskis, E. J., Munsat, T., Valdmanis, P., Rouleau, G. A., Hosler, B. A., Cortelli, P., de Jong, P. J., Yoshinaga, Y., Haines, J. L., Pericak-Vance, M. A., Yan, J., Ticozzi, N., Siddique, T., McKenna-Yasek, D., Sapp, P. C., Horvitz, H. R., Landers, J. E., and Brown, R. H., Jr. (2009) Mutations in the *FUS/TLS* gene on chromosome 16 cause familial amyotrophic lateral sclerosis. *Science* **323**, 1205–1208
- Vance, C., Rogelj, B., Hortobágyi, T., De Vos, K. J., Nishimura, A. L., Sreedharan, J., Hu, X., Smith, B., Ruddy, D., Wright, P., Ganesalingam, J., Williams, K. L., Tripathi, V., Al-Saraj, S., Al-Chalabi, A., Leigh, P. N., Blair, I. P., Nicholson, G., de Belleruche, J., Gallo, J. M., Miller, C. C., and Shaw, C. E. (2009) Mutations in FUS, an RNA processing protein, cause familial amyotrophic lateral sclerosis type 6. *Science* **323**, 1208–1211
- Iko, Y., Kodama, T. S., Kasai, N., Oyama, T., Morita, E. H., Muto, T., Okumura, M., Fujii, R., Takumi, T., Tate, S., and Morikawa, K. (2004) Domain architectures and characterization of an RNA-binding protein, TLS. *J. Biol. Chem.* **279**, 44834–44840
- Lee, B. J., Cansizoglu, A. E., Süel, K. E., Louis, T. H., Zhang, Z., and Chook, Y. M. (2006) Rules for nuclear localization sequence recognition by karyopherin β 2. *Cell* **126**, 543–558
- Zhang, Z. C., and Chook, Y. M. (2012) Structural and energetic basis of ALS-causing mutations in the atypical proline-tyrosine nuclear localization signal of the Fused in Sarcoma protein (FUS). *Proc. Natl. Acad. Sci. U.S.A.* **109**, 12017–12021
- Dormann, D., Rodde, R., Edbauer, D., Bentmann, E., Fischer, I., Hruscha, A., Than, M. E., Mackenzie, I. R., Capell, A., Schmid, B., Neumann, M., and Haass, C. (2010) ALS-associated fused in sarcoma (FUS) mutations disrupt transportin-mediated nuclear import. *EMBO J.* **29**, 2841–2857
- Doi, H., Okamura, K., Bauer, P. O., Furukawa, Y., Shimizu, H., Kurosawa, M., Machida, Y., Miyazaki, H., Mitsui, K., Kuroiwa, Y., and Nukina, N. (2008) RNA-binding protein TLS is a major nuclear aggregate-interacting protein in huntingtin exon 1 with expanded polyglutamine-expressing cells. *J. Biol. Chem.* **283**, 6489–6500
- Cushman, M., Johnson, B. S., King, O. D., Gitler, A. D., and Shorter, J. (2010) Prion-like disorders. Blurring the divide between transmissibility and infectivity. *J. Cell Sci.* **123**, 1191–1201
- Kaech, S., and Banker, G. (2006) Culturing hippocampal neurons. *Nature Protocols* **1**, 2406–2415
- Misonou, H., and Trimmer, J. S. (2005) A primary culture system for biochemical analyses of neuronal proteins. *J. Neurosci. Methods* **144**, 165–173
- Sun, Z., Diaz, Z., Fang, X., Hart, M. P., Chesi, A., Shorter, J., and Gitler, A. D. (2011) Molecular determinants and genetic modifiers of aggregation and toxicity for the ALS disease protein FUS/TLS. *PLoS Biol.* **9**, e1000614
- Ticozzi, N., Silani, V., LeClerc, A. L., Keagle, P., Gellera, C., Ratti, A., Taroni, F., Kwiatkowski, T. J., Jr., McKenna-Yasek, D. M., Sapp, P. C., Brown, R. H., Jr., and Landers, J. E. (2009) Analysis of *FUS* gene mutation in familial amyotrophic lateral sclerosis within an Italian cohort. *Neurology* **73**, 1180–1185
- Corrado, L., Del Bo, R., Castellotti, B., Ratti, A., Cereda, C., Penco, S., Sorarù, G., Carlomagno, Y., Ghezzi, S., Pensato, V., Colombrita, C., Gagliardi, S., Cozzi, L., Orsetti, V., Mancuso, M., Siciliano, G., Mazzini, L., Comi, G. P., Gellera, C., Ceroni, M., D'Alfonso, S., and Silani, V. (2010) Mutations of *FUS* gene in sporadic amyotrophic lateral sclerosis. *J. Med. Genet.* **47**, 190–194
- Van Langenhove, T., van der Zee, J., Sleegers, K., Engelborghs, S., Vandenberghe, R., Gijssels, I., Van den Broeck, M., Mattheijssens, M., Peeters, K., De Deyn, P. P., Cruts, M., and Van Broeckhoven, C. (2010) Genetic contribution of FUS to frontotemporal lobar degeneration. *Neurology* **74**, 366–371
- Bäumer, D., Hilton, D., Paine, S. M., Turner, M. R., Lowe, J., Talbot, K., and Ansorge, O. (2010) Juvenile ALS with basophilic inclusions is a FUS proteinopathy with FUS mutations. *Neurology* **75**, 611–618
- Huang, E. J., Zhang, J., Geser, F., Trojanowski, J. Q., Strober, J. B., Dickson, D. W., Brown, R. H., Jr., Shapiro, B. E., and Lomen-Hoerth, C. (2010) Extensive FUS-immunoreactive pathology in juvenile amyotrophic lateral sclerosis with basophilic inclusions. *Brain Pathol.* **20**, 1069–1076
- Bigio, E. H., Wu, J. Y., Deng, H. X., Bit-Ivan, E. N., Mao, Q., Ganti, R., Peterson, M., Siddique, N., Geula, C., Siddique, T., and Mesulam, M. (2013) Inclusions in frontotemporal lobar degeneration with TDP-43 proteinopathy (FTLD-TDP) and amyotrophic lateral sclerosis (ALS), but not FTLD with FUS proteinopathy (FTLD-FUS), have properties of amyloid. *Acta Neuropathol.* **125**, 463–465
- Bosco, D. A., Lemay, N., Ko, H. K., Zhou, H., Burke, C., Kwiatkowski, T. J., Jr., Sapp, P., McKenna-Yasek, D., Brown, R. H., Jr., and Hayward, L. J. (2010) Mutant FUS proteins that cause amyotrophic lateral sclerosis incorporate into stress granules. *Hum. Mol. Genet.* **19**, 4160–4175
- Gal, J., Zhang, J., Kwinter, D. M., Zhai, J., Jia, H., Jia, J., and Zhu, H. (2011) Nuclear localization sequence of FUS and induction of stress granules by ALS mutants. *Neurobiol. Aging* **32**, 2323.e27–2323.e40
- Avila, J. (1992) Microtubule functions. *Life Sci.* **50**, 327–334
- Kitagawa, K., Matsumoto, M., Niinobe, M., Mikoshiba, K., Hata, R., Ueda, H., Handa, N., Fukunaga, R., Isaka, Y., and Kimura, K. (1989) Microtubule-associated protein 2 as a sensitive marker for cerebral ischemic damage. Immunohistochemical investigation of dendritic damage. *Neuroscience* **31**, 401–411
- Springer, J. E., Azbill, R. D., Kennedy, S. E., George, J., and Geddes, J. W. (1997) Rapid calpain I activation and cytoskeletal protein degradation following traumatic spinal cord injury. Attenuation with riluzole pretreatment. *J. Neurochem.* **69**, 1592–1600
- Taft, W. C., Yang, K., Dixon, C. E., and Hayes, R. L. (1992) Microtubule-associated protein 2 levels decrease in hippocampus following traumatic brain injury. *J. Neurotrauma* **9**, 281–290
- Polymenidou, M., and Cleveland, D. W. (2011) The seeds of neurodegeneration. Prion-like spreading in ALS. *Cell* **147**, 498–508
- Harper, J. D., and Lansbury, P. T., Jr. (1997) Models of amyloid seeding in Alzheimer's disease and scrapie: mechanistic truths and physiological consequences of the time-dependent solubility of amyloid proteins. *Annu. Rev. Biochem.* **66**, 385–407
- Zinszner, H., Albalat, R., and Ron, D. (1994) A novel effector domain from the RNA-binding protein TLS or EWS is required for oncogenic transformation by CHOP. *Genes Dev.* **8**, 2513–2526
- Prasad, D. D., Ouchida, M., Lee, L., Rao, V. N., and Reddy, E. S. (1994) TLS/FUS fusion domain of TLS/FUS-erg chimeric protein resulting from the t(16;21) chromosomal translocation in human myeloid leukemia functions as a transcriptional activation domain. *Oncogene* **9**, 3717–3729
- Han, T. W., Kato, M., Xie, S., Wu, L. C., Mirzaei, H., Pei, J., Chen, M., Xie, Y., Allen, J., Xiao, G., and McKnight, S. L. (2012) Cell-free formation of RNA granules. Bound RNAs identify features and components of cellular assemblies. *Cell* **149**, 768–779
- Kato, M., Han, T. W., Xie, S., Shi, K., Du, X., Wu, L. C., Mirzaei, H., Goldsmith, E. J., Longgood, J., Pei, J., Grishin, N. V., Frantz, D. E., Schneider, J. W., Chen, S., Li, L., Sawaya, M. R., Eisenberg, D., Tycko, R., and McKnight, S. L. (2012) Cell-free formation of RNA granules. Low complexity sequence domains form dynamic fibers within hydrogels. *Cell* **149**, 753–767
- Hicks, G. G., Singh, N., Nashabi, A., Mai, S., Bozek, G., Klewes, L., Arapovic, D., White, E. K., Koury, M. J., Oltz, E. M., Van Kaer, L., and Ruley, H. E. (2000) FUS deficiency in mice results in defective B-lymphocyte development and activation, high levels of chromosomal instability and peri-

- natal death. *Nat. Genet.* **24**, 175–179
35. Lagier-Tourenne, C., Polymenidou, M., and Cleveland, D. W. (2010) TDP-43 and FUS/TLS. Emerging roles in RNA processing and neurodegeneration. *Hum. Mol. Genet.* **19**, R46–R64
36. Ishigaki, S., Masuda, A., Fujioka, Y., Iguchi, Y., Katsuno, M., Shibata, A., Urano, F., Sobue, G., and Ohno, K. (2012) Position-dependent FUS-RNA interactions regulate alternative splicing events and transcriptions. *Scientific Reports* **2**, 529
37. Fujioka, Y., Ishigaki, S., Masuda, A., Iguchi, Y., Udagawa, T., Watanabe, H., Katsuno, M., Ohno, K., and Sobue, G. (2013) FUS-regulated region- and cell-type-specific transcriptome is associated with cell selectivity in ALS/FTLD. *Scientific Reports* **3**, 2388
38. Orozco, D., Tahirovic, S., Rentzsch, K., Schwenk, B. M., Haass, C., and Edbauer, D. (2012) Loss of fused in sarcoma (FUS) promotes pathological Tau splicing. *EMBO Rep.* **13**, 759–764
39. Lee, V. M., Goedert, M., and Trojanowski, J. Q. (2001) Neurodegenerative tauopathies. *Annu. Rev. Neurosci.* **24**, 1121–1159
40. Phukan, J., Pender, N. P., and Hardiman, O. (2007) Cognitive impairment in amyotrophic lateral sclerosis. *Lancet Neurol.* **6**, 994–1003
41. DeJesus-Hernandez, M., Kocerha, J., Finch, N., Crook, R., Baker, M., Desaro, P., Johnston, A., Rutherford, N., Wojtas, A., Kennelly, K., Wszolek, Z. K., Graff-Radford, N., Boylan, K., and Rademakers, R. (2010) *De novo* truncating FUS gene mutation as a cause of sporadic amyotrophic lateral sclerosis. *Hum. Mutat.* **31**, E1377–E1389
42. Groen, E. J., van Es, M. A., van Vught, P. W., Spliet, W. G., van Engelen-Lee, J., de Visser, M., Wokke, J. H., Schelhaas, H. J., Ophoff, R. A., Fumoto, K., Pasterkamp, R. J., Dooijes, D., Cuppen, E., Veldink, J. H., and van den Berg, L. H. (2010) FUS mutations in familial amyotrophic lateral sclerosis in the Netherlands. *Arch. Neurol.* **67**, 224–230
43. Hewitt, C., Kirby, J., Highley, J. R., Hartley, J. A., Hibberd, R., Hollinger, H. C., Williams, T. L., Ince, P. G., McDermott, C. J., and Shaw, P. J. (2010) Novel FUS/TLS mutations and pathology in familial and sporadic amyotrophic lateral sclerosis. *Arch. Neurol.* **67**, 455–461
44. Robertson, J., Bilbao, J., Zinman, L., Hazrati, L. N., Tokuhira, S., Sato, C., Moreno, D., Strome, R., Mackenzie, I. R., and Rogaeva, E. (2011) A novel double mutation in FUS gene causing sporadic ALS. *Neurobiol. Aging* **32**, 553.e27–553.e30
45. Suzuki, N., Aoki, M., Warita, H., Kato, M., Mizuno, H., Shimakura, N., Akiyama, T., Furuya, H., Hokonohara, T., Iwaki, A., Togashi, S., Konno, H., and Itoyama, Y. (2010) FALS with FUS mutation in Japan, with early onset, rapid progress and basophilic inclusion. *J. Hum. Genet.* **55**, 252–254
46. Waibel, S., Neumann, M., Rabe, M., Meyer, T., and Ludolph, A. C. (2010) Novel missense and truncating mutations in FUS/TLS in familial ALS. *Neurology* **75**, 815–817
47. Yan, J., Deng, H. X., Siddique, N., Fecto, F., Chen, W., Yang, Y., Liu, E., Donkervoort, S., Zheng, J. G., Shi, Y., Ahmeti, K. B., Brooks, B., Engel, W. K., and Siddique, T. (2010) Frameshift and novel mutations in FUS in familial amyotrophic lateral sclerosis and ALS/dementia. *Neurology* **75**, 807–814

Intranuclear Aggregation of Mutant FUS/TLS as a Molecular Pathomechanism of Amyotrophic Lateral Sclerosis

Takao Nomura, Shoji Watanabe, Kumi Kaneko, Koji Yamanaka, Nobuyuki Nukina and Yoshiaki Furukawa

J. Biol. Chem. 2014, 289:1192-1202.

doi: 10.1074/jbc.M113.516492 originally published online November 26, 2013

Access the most updated version of this article at doi: [10.1074/jbc.M113.516492](https://doi.org/10.1074/jbc.M113.516492)

Alerts:

- [When this article is cited](#)
- [When a correction for this article is posted](#)

[Click here](#) to choose from all of JBC's e-mail alerts

This article cites 47 references, 13 of which can be accessed free at <http://www.jbc.org/content/289/2/1192.full.html#ref-list-1>